Effects of nanocasting parameters on surface area properties of PEG 400-based ordered mesoporous carbon

Cite as: AIP Conference Proceedings **2124**, 020035 (2019); https://doi.org/10.1063/1.5117095
Published Online: 24 July 2019

A. Afandi, M. A. Ahmad, B. H. Hameed, et al.

Effects of Nanocasting Parameters on Surface Area Properties of PEG 400-Based Ordered Mesoporous Carbon

A. Afandi, M. A. Ahmad, B. H. Hameed, and A. T. Mohd Din [a)]

School of Chemical Engineering, Engineering Campus, Universiti Sains Malaysia,
14300 Nibong Tebal Penang, Malaysia

[a)]Corresponding author: chazam@usm.my

Abstract. In this work, ordered mesoporous carbon (OMC) was synthesised via the nanocasting process using hexagonal mesoporous silica (HMS) as the template and polyethylene glycol 400 (PEG 400) as the carbon precursor by varying four vital process conditions, namely, carbonisation temperature, dwelling time, heating rate, and carbon loading. The best conditions were selected based on the ability of the OMC samples to remove methylene blue (MB). ABA-16 exhibited the highest total surface area (1,020 $m^2.g^{-1}$) with its pore diameter measured at 3.89 nm, and a total pore volume of 0.9976 $cm^3.g^{-1}$. It was prepared using 2.5 g of PEG 400 per gram of HMS, carbonised at 800 °C, with a heating rate of 1°C.min^{-1}, and 240 min of dwelling time. A series of batch adsorption tests was conducted on MB at different initial concentrations at 30– 50 °C. The maximum MB adsorption capacity, Q_m was at 394.88 $mg.g^{-1}$ at 303 K. For all tested conditions, Freundlich produced better fittings than Langmuir isotherm model. All these findings suggested that nanocasting parameters play important roles in producing functional OMC with good physicochemical properties for the removal of pollutants from water bodies.

1.0 INTRODUCTION

Various treatment methods have been employed for the removal of micropollutants from wastewater. However, the adsorption technique was found to be superior to other removal methods. Ordered mesoporous carbon (OMC) recently attracted significant scientific interests because of its high specific area, large pore volume, unique intrinsic structures, chemical inertness, and tunable pore size. Due to its advantageous properties, OMC is a promising adsorbent for a vast application area, which includes removal of micropollutants from wastewater [1, 2], as a nanoparticle-based drug delivery system [3], as an environmental adsorbent [4], and as a supercapasitor [5].

To enhance the adsorption ability of OMC, recent research attention has been focused on synthesising OMC with tunable pore structure, suitable for effective adsorption of materials with larger molecular size. The adsorption ability of OMC is mainly determined by its physicochemical properties, such as surface chemistry and porosity. These properties can be controlled using the process parameters, such as carbonisation temperature, dwelling time, heating rate, and carbon loading. Recently, a new OMC was synthesised using SBA-15 as the template and m-diethylbenzene as the carbon source, with maximum surface area of 1,044 $m^2.g^{-1}$ and total pore volume of 1.20 $cm^3.g^{-1}$, which was obtained at carbonisation temperature of 800 °C [6]. The choice of the carbon source also plays a vital role based on availability, economical aspect, non-edible, and environmentally friendly. OMCs with total surface areas ranging between 384 and 469 $m^2.g^{-1}$ have been synthesised using SBA-15 as the template and acrylic acid as the carbon source [7]. Meanwhile, OMC with an improved surface area of 724 $m^2.g^{-1}$ was previously prepared using SBA-15 template and 2,3-dihydroxynaphtalene as the carbon source [8].

The objective of this study was to synthesise OMC samples via the nanocasting (also known as hard-templating) method using HMS as the template and non-edible PEG 400 as the liquid carbon source. The effects of carbonisation temperature, dwelling time, heating rate, and PEG 400 loading on the mesoporous structure, yield, total surface area, pore volume, and surface morphology of the samples were studied. The best operating condition was picked after each parameter has been screened and held constant during each set of experiments. The selection was determined based on the ability of each OMC sample to adsorb MB as a meso-sized model solute, with a compromise on the collected carbon yields to reflect an important economical aspect in the manufacturing point of view.

6th International Conference on Environment (ICENV2018)
AIP Conf. Proc. 2124, 020035-1–020035-11; https://doi.org/10.1063/1.5117095
Published by AIP Publishing. 978-0-7354-1864-6/$30.00

2.0 MATERIALS AND METHODS

2.1 Materials

Pluronic 123 was used to prepare the HMS template and tetraethyl orthosilicate (TEOS, 98%) was used as the silica source. Hydrochloric acid (HCl, 37%), sodium hydroxide (NaOH, 98%), and methylene blue (MB) were all purchased from Sigma Aldrich. Sulphuric acid (H_2SO_4, 95–97%) and polyethylene glycol 400 (PEG 400) were purchased from Merck.

2.2 Preparation of Hexagonal Mesoporous Silica

The template material was synthesised using a tri-block copolymer template (Pluronic 123), as described by Zhou et al. [9]. First, 450 mL of 2.5 M HCl solution was prepared and mixed with 12 g of Pluronic 123 in a 1,000 mL glass beaker. The mixture was placed on a magnetic hot plate and stirred at 650 RPM. Once the solution became clear and colourless, 23 g of tetraethyl orthosilicate (TEOS) was slowly introduced to the solution. The colour of the mixture gradually turned from cloudy to white in 2 h. The beaker was then placed into a water bath shaker and left for aging for 48 h. The temperature of the whole process was maintained at around 308 to 313 K. The resultant white precipitate was collected through filtration. The process of washing the precipitate with deionised water was repeated several times to remove impurities. The obtained white solid cake was left to dry at room temperature for 48 h. Then, the dried cake was calcined in a muffle furnace at 823 K, with a heating rate of 1 $K.min^{-1}$, and dwelling time of 4 h. The obtained white silica was in powder form and was kept in an air tight container for further usage.

2.3 Nanocasting of Ordered Mesoporous Carbon

Ordered mesoporous carbon was prepared through the nanocasting method. First, 1.0 g of HMS was added into a known amount of PEG 400 in a 100 mL ceramic crucible. A small amount of pure H_2SO_4 was then poured into the mixture. It was thoroughly mixed at room temperature (303 K) until the mixture turned into a dark-brown colour. The mixture was then placed in an oven at 100 °C for 24 h for partial carbonisation and drying purposes. The resulting sticky black mixture was sent for thermal treatment at the designated carbonisation temperatures, heating rates, and dwelling time using a fabricated pyrolysis furnace, embedded with a proportional integral derivative (PID) micro-controller (Model PXR-4, Fuji Electric, Japan). Nitrogen flow (50 $cm^3.min^{-1}$) was kept constant throughout the carbonisation process. The resultant carbon-silica composite was washed with 1.0 M NaOH solution at elevated temperature to remove the silica template. Finally, the obtained carbon sample was filtered, washed, and dried until further use. OMC material yield (%) was calculated based on the following Eq. (1):

$$Yield,\% = \frac{m_{omc}}{m_{cp}} x100 \quad (1)$$

where, m_{omc} is the dry mass of the OMC sample recovered from the template (g), and m_{cp} is the mass of organic carbon precursor introduced to the template (g).

2.4 Effect of Carbonisation Temperature

The carbonisation temperature was varied at 600, 650, 700, 750, and 800 °C, while other parameters were held constant (dwelling time: 60 min, heating rate: 1 $°C.min^{-1}$, PEG 400 loading: 5 g).

2.5 Effect of Dwelling Time

The dwelling time was varied at 15, 30, 60, 120, and 240 minutes, while other parameters were held constant (carbonisation temperature: 800 °C, heating rate: 1 $°C.min^{-1}$, PEG 400 loading: 5 g).

2.6 Effect of Heating Rate

The heating rate was varied at 1, 2.5, 5, 7.5, and 10 °C.min^{-1}, while other parameters were held constant (carbonisation temperature: 800 °C, dwelling time: 240 min, PEG 400 loading: 5 g).

2.7 Effect of Polyethylene Glycol 400 Loading

The PEG 400 loading was varied from 2.5, 5, 7.5, 10, and 15 g per g of HMS, while other parameters were held constant (carbonisation temperature: 800 °C, dwelling time: 240 min, heating rate: 1 °C.min^{-1}). Accordingly, the synthesised samples were named using the following code; ABA-n. ABA stands for Azam-Bassim-Azmier, while 'n' represents the sequence number of the respective runs. Table 1 summarises the one-time variable experimental approach in nanocasting of ordered mesoporous carbon.

Table 1: Operating conditions for nanocasting of ordered mesoporous carbon samples

Sample	Temperature (°C)	Dwelling time (min)	Heating rate (°C.min^{-1})	PEG 400 loading (g)
ABA-1	600	60	1	5
ABA-2	650	60	1	5
ABA-3	700	60	1	5
ABA-4	750	60	1	5
ABA-5	800	60	1	5
ABA-6	800	15	1	5
ABA-7	800	30	1	5
ABA-8	800	60	1	5
ABA-9	800	120	1	5
ABA-10	800	240	1	5
ABA-11	800	240	1	5
ABA-12	800	240	2.5	5
ABA-13	800	240	5	5
ABA-14	800	240	7.5	5
ABA-15	800	240	10	5
ABA-16	800	240	1	2.5
ABA-17	800	240	1	5.0
ABA-18	800	240	1	7.5
ABA-19	800	240	1	10.0
ABA-20	800	240	1	15.0

2.8 Characterisation

The surface area, pore volume, and pore size distribution properties were measured using nitrogen adsorption, in an accelerated surface area and porosimetry system, ASAP 2020 (Micromeritics, USA). The sample was degassed for 8 h under vacuum at 300 °C prior to the analysis. After degassing, the sample was transferred to the analysis system where it was cooled in liquid nitrogen. A multipoint analysis was conducted at -196.15 °C to obtain the nitrogen adsorption-desorption isotherm by admitting successive known volumes of nitrogen in and out of the sample and measuring the equilibrium pressure. The adsorption isotherm was obtained by measuring the quantities of gas removed from the sample as the relative pressure integrated with the instrument. Calculations of total surface area and average pore size measurements were performed using the user-friendly ASAP 2020 software.

2.9 Batch Adsorption Studies

To select an optimum adsorbent, 0.1 g of each ABA-n sample was added into a conical flask containing 100 mL of known initial MB concentration and covered with a glass stopper. The conical flasks were placed in a water bath at 30–50 °C until equilibrium was reached. Samples were taken and filtered, and the MB concentration was analysed using a UV-visible spectrophotometer at the maximum wavelength of 665 nm. The removal percentage of MB was obtained using the following Equation (2):

$$Removal\ (\%) = \frac{C_0 - C_e}{C_0} \times 100 \qquad (2)$$

where C_0 and C_e are the initial and equilibrium dye concentrations (mg/L), respectively. C_t is the dye concentration at time t (mg/L). V is the volume of the solution (L), and w is the mass of the adsorbents (g).

3.0 RESULTS AND DISCUSSION

3.1 Effect of Carbonisation Temperature

Temperature can greatly influence the carbonisation process of products, particularly on carbon yield and porosity. In general, higher carbon yields are observed at lower temperature range due to lower burn-off degree. In the meantime, lower carbon yields are collected at higher temperature range as the materials would often suffer from high burn-off. Figure 1 shows the decreasing trend of the carbon yield against increasing carbonization temperature.

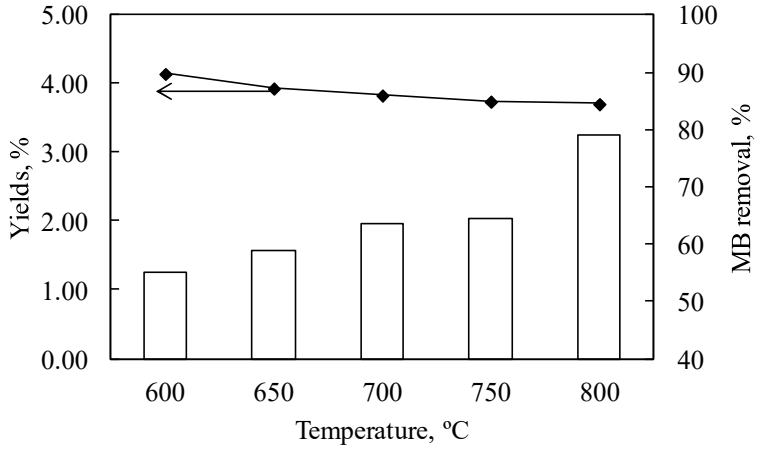

Fig 1: Effect of carbonization temperature on carbon yield and MB removal percentage

The mass of the carbon had consistently dropped from 0.2073 g (600 ºC) to 0.1853 g (800 ºC). The trend represents approximately 10% drop in the mass of collected carbon across the increasing temperature range. Such trend was expected due to moisture loss and thermal degradation of the volatile organic substances in the HMS/PEG 400 mixtures. A similar observation was made during the preparation of activated carbon from cassava peels at different carbonisation temperatures [10]. Stable carbon yields were observed when carbonisation was performed at higher than 700 ºC. This was because the volatile organic compounds were almost entirely degraded from the mixture of carbon precursors at that particular range of temperature [11]. The increasing MB uptakes using samples prepared at higher temperatures were also observed. Table 2 lists the surface area properties for the selected samples. The total surface area had decreased with increasing temperature. The highest total surface area was 843.72 $m^2.g^{-1}$, prepared at 600 °C, while the smallest total surface area was 800.30 $m^2.g^{-1}$, prepared at 800 °C.

Table 2: Surface area properties of ordered mesoporous carbons prepared at different carbonisation temperatures.

Sample	Carbonisation temperature[1]	BET surface area[2]	Micropore surface area[3]	Total pore volume[4]	Micropore volume[5]	Average pore diameter[6]
ABA-1	600	843.72	250.55	0.5684	0.1237	2.695
ABA-2	650	825.38	252.99	0.5549	0.1245	2.641
ABA-3	700	839.73	239.51	0.5717	0.1179	2.723
ABA-4	750	804.11	277.67	0.5326	0.1393	2.750
ABA-5	800	800.30	259.85	0.5368	0.1308	2.683

[1]Carbonisation temperature (°C), [2]BET surface area ($m^2.g^{-1}$), [3]T-plot micropore surface area ($m^2.g^{-1}$), [4]Total pore volume ($cm^3.g^{-1}$), [5]Micropore volume ($cm^3.g^{-1}$), and [6]BET average pore diameter 4V/A (nm)

ABA-5 demonstrated up to 79.1% of MB removal, in equivalent to 197.8 $mg.g^{-1}$ of MB uptake. In comparison, ABA-1 achieved 137.6 $mg.g^{-1}$ of MB uptake under similar adsorption conditions. Based on Figure 2, no definite correlations were found between the amount of MB uptake and the presented surface area properties of the OMC samples. However, some findings suggested that the active functional groups in the carbon prepared at various temperatures might be the possible cause for such occurrence. C=O and C-O groups can be easily destructed at high carbonisation temperature [12]. Similarly, O-H from the carboxylic group would also decompose at a higher temperature [13]. However, carbonisation temperature of 800 °C was chosen as the optimum temperature since this decision was based on the key criteria; the best ability of the adsorbent to remove MB from aqueous phase.

3.2 Effect of Dwelling Time

The variations in the OMC yield, prepared at different dwelling times ranging from 15 to 240 minutes, are presented in Figure 2. The figure shows that dwelling time of longer than 30 minutes has contributed to a higher weight loss of carbon, and thus, translated into a lesser carbon yield. The carbon yields were decreased from 4.6 to 3.7% when the dwelling time was extended to 60 minutes. However, the decreasing yield became stabilised when the dwelling time was extended further, up to 240 minutes (3.5%). Such trend is inevitable due to prolonged pyrolytic effect on carbonaceous materials. ABA-10 possessed the lowest micropore volume of 0.0943 $cm^3.g^{-1}$, relative to the rest of the samples (refer Table 3). Therefore, prolonged dwelling time can lead to significant destruction of the structure of the microspores, yet simultaneously improving the mesoporosity. The lowest micropore surface area of 188.45 $m^2.g^{-1}$ was observed in ABA-10, which dwelled under heat for 240 minutes. The small pores were unable to withstand the heat stress for such period of time. The walls of the pores began to expand and finally collapsed, resulting in larger and wider pores. Consequently, a decrease in the total surface area of the carbonised sample was observed.

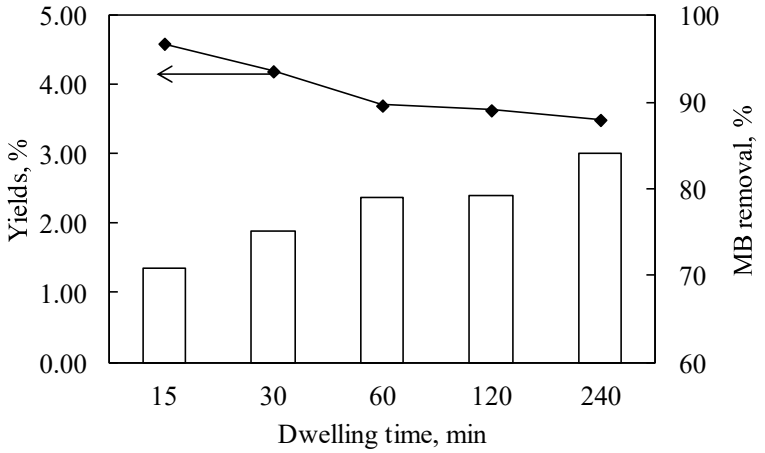

Fig 2: Effect of dwelling time on carbon yields and MB removal percentage

Table 3: Surface area properties of ordered mesoporous carbon samples prepared at different dwelling times.

Sample	Dwelling time[1]	BET surface area[2]	Micropore surface area[3]	Total pore volume[4]	Micropore volume[5]	Average pore diameter[6]
ABA-6	15	692.64	220.76	0.5119	0.1112	2.956
ABA-7	30	754.89	202.76	0.5190	0.1021	2.750
ABA-8	60	800.30	259.85	0.5368	0.1308	2.683
ABA-9	120	731.10	272.90	0.4767	0.1369	2.608
ABA-10	240	673.210	188.45	0.4219	0.0943	2.507

[1]Dwelling time (min), [2]BET surface area ($m^2.g^{-1}$), [3]T-plot micropore surface area ($m^2.g^{-1}$), [4]Total pore volume ($cm^3.g^1$), [5]Micropore volume ($cm^3.g^{-1}$) and [6]BET average pore diameter 4V/A (nm)

Meanwhile, a short dwelling time of 15 min for ABA-6 seemed to be insufficient and immature. As a result, ABA-6 recorded the least MB removal percentage of approximately 71%. Even though the dwelling time of 2 hours has produced an OMC sample with the highest surface area properties, the MB removal performance shown by ABA-8 was slightly lower than ABA-10.

The overall surface area properties were enhanced when the dwelling time of 15 minutes was prolonged up to 60 minutes. However, the detrimental effect on the surface area properties was noticeable when dwelling time was extended to 240 minutes. According to [14], this could be due to the increased softening of some volatile fractions, forming an immediate melt that closed and sealed some of the pores. This condition has contributed to a significant reduction in pore surface area. It is proposed that longer carbonisation time has encouraged the formation of functional surface groups that are beneficial for higher MB removal using ABA-10. This could be one of the possible reasons that contribute to higher MB uptakes using ABA-10. Therefore, a period of 240 minutes has been selected as the best dwelling time for nanocasting OMC in this study.

3.3 Effect of Heating Rate

Heating rate is another key parameter that could influence the porosity of the synthesised material. The rate of thermal heating, either low or high, could significantly affect the pore size and its distributions. Figure 3 shows significant correlations between carbon yield and MB removal percentage when heating rates were varied at the designated values. A summary of the surface area properties of ABA-11, ABA-12, ABA-13, ABA-14, and ABA-15 is presented in Table 4. The mass of the obtained carbon samples had gradually decreased from approximately 0.200 g at heating rates of 7.5 and 10 °C.min^{-1} to 0.175 g when the heating rate was decreased to 1 ºC.min^{-1}. It is possible that at low heating rate, the time required for the furnace to achieve the desired temperature would be longer and thus, exposing the material to a longer thermal degradation process. ABA-11, prepared at the lowest heating rate of 1 ºC.min^{-1}, exhibited the highest MB removal of 84%. The other samples had shown a much lower MB removal percentage. A decrease of more than 10% of MB removal percentage was observed when heating rates of higher than 2.5 ºC.min^{-1} were applied throughout the experiments. It was found that the increased heating rate, from 1 to 10 °C.min^{-1}, had reduced the total surface area of all OMC samples, with the exception of ABA-14.

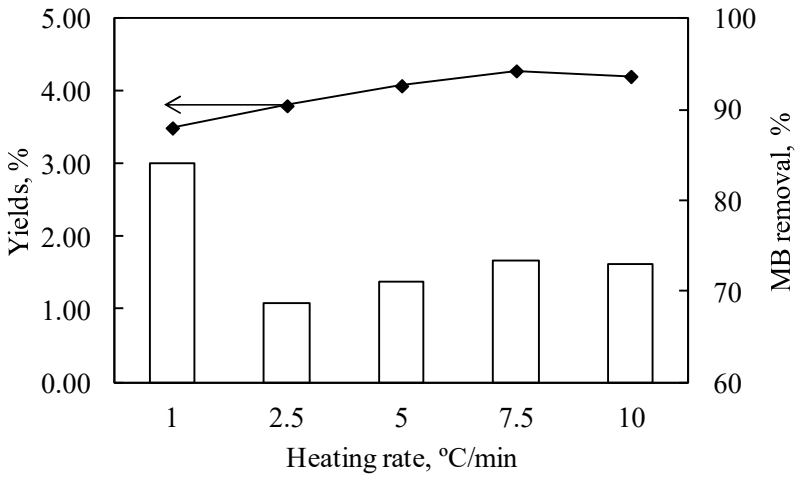

Fig 3: Effect of heating rate on carbon yields and MB removal percentage

Table 4: Surface area properties of ordered mesoporous carbon samples prepared at different heating rates

Sample	Heating rate[1]	BET surface area[2]	Micropore surface area[3]	Total pore volume[4]	Micropore volume[5]	Average pore diameter[6]
ABA-11	1	673.21	188.45	0.4219	0.0943	2.507
ABA-12	2.5	548.09	334.55	0.3048	0.1653	2.225
ABA-13	5	449.26	223.28	0.2649	0.1092	2.358
ABA-14	7.5	673.47	289.07	0.4218	0.1444	2.505
ABA-15	10	573.84	223.85	0.3680	0.1100	2.565

[1]Heating rate (°C/min), [2]BET surface area ($m^2.g^{-1}$), [3]T-plot micropore surface area ($m^2.g^{-1}$), [4]Total pore volume ($cm^3.g^{-1}$), [5]Micropore volume ($cm^3.g^{-1}$) and [6]BET average pore diameter 4V/A (nm)

Various findings on the effect of heating rate on carbon materials have been reported in the literature. The surface area of activated carbon prepared from lignite was found to be the highest when prepared at the slowest heating rate of 5 ºC.min^{-1} [15]. Further increase in heating rate, up to 20 °C.min^{-1}, has caused insignificant differences on the yield and surface area properties of the carbons. On the other hand, carbon materials synthesised at quicker heating rates have shown higher reactivity and better surface area properties compared to those subjected to slow heating rates [16]. In this study, a heating rate of 1 °C/min^{-1} was chosen for the commencement of the next parametric studies based on the excellent MB removal performance and better surface area properties shown by ABA-11.

3.4 Effect of Polyethylene Glycol 400 Loading

Figure 4 presents the relationships between carbon yield and MB removal over variations in PEG 400 loading. An initial precursor loading of 2.5 g per g template in ABA-16 has resulted in a high carbon yield of 0.1325 g. Further increases in loading of up to 15 g PEG 400 per g template have produced higher mass of carbon, but with decreased yield percentage. Excessive carbon precursor during the infiltration stage could have caused blockage in the pores of the template. Therefore, only a substantial amount of carbon molecules could have infiltrated the pores, leaving the remaining carbon on the template surface. The carbon molecules on the surface could be negatively affected by thermal degradation. Meanwhile, the carbon molecules that have successfully attached inside the pores would be better protected from aggressive degradation. Thus, this would allow the carbon molecules to form crystallites in a rigid skeletal structure similar to the template.

According to Table 5, an increase in PEG 400 loading has resulted in the decreased values of surface area, pore volume, and average pore diameter. Samples with lower PEG 400 loadings (ABA-16 and ABA-17) have demonstrated MB removal percentages of higher than 80 % compared to ABA-18, ABA-19, and ABA-20. The MB removal results were consistent with the characterised surface area properties of the synthesised samples,

whereby the use of higher loadings of PEG 400 has caused decreases in total surface area and total pore volume. Table 5 presents the surface area properties of the prepared carbons at different PEG 400 loadings. The optimum PEG 400 loading in this study was 2.5 g of PEG 400 per 1 g of HMS template.

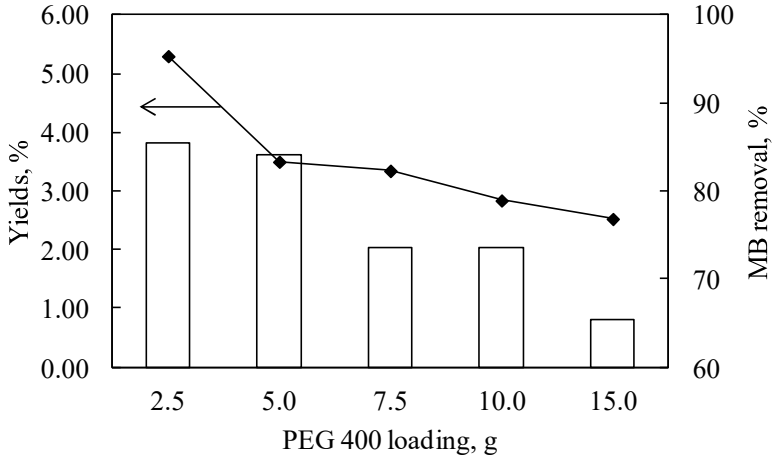

Fig 4: Effect of PEG 400 loading on carbon yields and MB removal percentage

Table 5: Surface area properties of ordered mesoporous carbon samples prepared at different PEG 400 loadings

Sample	PEG 400 loading[1]	BET surface area[2]	Micropore surface area[3]	Total pore volume[4]	Micropore volume[5]	Average pore diameter[6]
ABA-16	2.5	1026.02	399.89	0.9976	0.1927	3.889
ABA-17	5.0	673.21	188.45	0.4219	0.0943	2.507
ABA-18	7.5	675.33	323.28	0.4211	0.1608	2.494
ABA-19	10.0	592.45	347.29	0.3426	0.1719	2.312
ABA-20	15.0	464.83	117.15	0.3731	0.0550	3.210

[1]PEG 400 loading (g), [2]BET surface area ($m^2.g^{-1}$), [3]T-plot micropore surface area ($m^2.g^{-1}$), [4]Total pore volume ($cm^3.g^{-1}$), [5]Micropore volume ($cm^3.g^{-1}$) and [6]BET average pore diameter 4V/A (nm)

3.5 Methylene Blue Adsorption

A methylene blue adsorption profile at 30 °C using ABA-16 is presented in Figure 5. Equilibrium time of 30 minutes was reached for a 50 $mg.L^{-1}$ solution compared to 60 and 180 minutes for 150 $mg.L^{-1}$ and 500 $mg.L^{-1}$ solutions, respectively. The corresponding equilibriums for MB removal were 49.03, 144.77, and 404.47 $mg.g^{-1}$ with respect to initial concentrations of 50, 150, and 500 $mg.L^{-1}$ of MB solutions. The initial rapid phase within the first 5 min could be due to the high number of vacant sites available at the initial stage [17]. Furthermore, the rate of adsorption had increased with the increase in initial dye concentration, which could probably be due to the driving force [17]. In agreement with Peng et al. (2014), the adsorption profile of MB had increased from 165 to 358 $mg.g^{-1}$ when MB concentration was increased from 100 to 200 $mg.L^{-1}$ [18]. Thus, this smooth and continuous adsorption curve leading to saturation indicated the possibility of a monolayer coverage on the surface of the adsorbent by MB molecules [18].

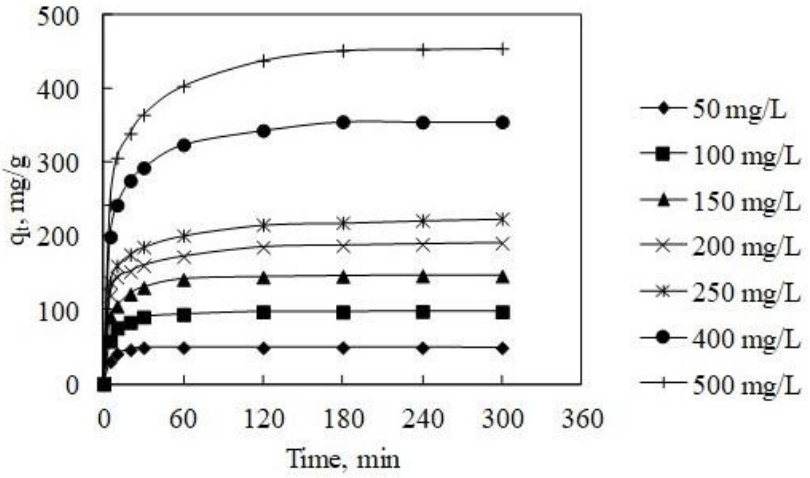

Fig. 5: Equilibrium profiles of MB adsorption using ABA-16 at 30 °C.

Table 6: Two-parameter isotherms and correlation coefficients for the adsorption of MB dyes using ABA-16.

Model	Temperature	Constants		r^2	ARE	MPSD
Langmuir	30 °C	K_L (L.mg^{-1})	0.081	0.9138	1.4735	0.4364
		Q_m (mg.g^{-1})	394.888			
		R_L	0.024			
	40 °C	K_L (L.mg^{-1})	0.057	0.9433	1.5461	0.5596
		Q_m (mg.g^{-1})	387.843			
		R_L	0.034			
	50 °C	K_L (L.mg^{-1})	0.055	0.9336	1.4050	0.4890
		Q_m (mg.g^{-1})	352.401			
		R_L	0.035			
Freundlich	30 °C	K_F (mg.g^{-1})(L.mg^{-1})$^{1/n}$	66.069	0.9697	0.8649	0.1638
		n	2.612			
	40 °C	K_F (mg.g^{-1})(L.mg^{-1})$^{1/n}$	60.143	0.9929	0.3943	0.0523
		n	2.674			
	50 °C	K_F (mg.g^{-1})(L.mg^{-1})$^{1/n}$	55.895	0.9849	0.5168	0.0573
		n	2.766			

3.6 Adsorption Isotherms

The equilibrium data for the adsorption of MB were fitted into two-parameter adsorption isotherm models. The adsorption equilibrium data of MB onto ABA-16 were analysed using Langmuir and Freundlich isotherm models. The parameter values of the respective isotherm models are listed in Table 6. The fittings on Langmuir model at 30, 40, and 50 °C have produced non-linear regression coefficients (r^2) of 0.9138, 0.9433, and 0.9336, respectively. The value of r^2 within the range of 0.9 to 1 indicates a good agreement between the experimental data and the mathematical equation that represents the Langmuir isotherm. The Q_m values representing the estimated Langmuir monolayer adsorption capacity had steadily decreased with increasing temperature. These trends infer that the adsorption of MB on the surface of ABA-16 was exothermic in nature. At 30 °C, the Q_m value was calculated at 394.89 mg.g^{-1}, and had further decreased to 387.84 and 352.40 mg.g^{-1} at 40 and 50 °C,

respectively. The K_L values of 0.081, 0.057, and 0.055 were close to zero. Further calculation of R_L using the values of K_L has shown that the adsorption of MB was favourable ($0 < R_L < 1$) and possibly reversible. MB molecules were assumed to be distributed in single layer coverage on the surface of ABA-16. The experimental data of MB adsorption on ABA-16 can also be represented by Freundlich based on stronger r^2 (0.9697-0.9929) values of closer to 1. The resultant ARE and MPSD values were also small. The values of K_F constant were found to decrease with decreasing temperature. The K_F values were 66.07, 60.14, and 55.89 (mg. g^{-1})(L.mg^{-1})$^{1/n}$ at 30, 40, and 50 °C, respectively. The surface heterogeneity represented by 1/n had decreased when the temperature was increased. A value closer to 0 would indicate an increasing surface heterogeneity of the adsorption system. A strong conformation of the experimental data to Freundlich model implied that MB molecules have a multilayer surface coverage on ABA-16.

4.0 CONCLUSION

This study has concluded that the synthesis of OMC was greatly influenced by the carbonisation process. Increases in temperature and dwelling time have resulted in lower OMC yields. Meanwhile, low heating rates have caused increased mass loss due to longer exposure to heat. ABA-16, which was synthesised at carbonisation temperature of 800 °C, dwelling time of 240 min, heating rate of 1 °C/min, and PEG 400 loading of 2.5 g, had exhibited the highest total surface area of 1026 $m^2.g^{-1}$ and the total pore volume of 0.9976 $cm^3.g^{-1}$. Then, the efficiency of this mesoporous carbon in removing methylene blue was examined. Freundlich isotherm model fitted well with the experimental data, with the adsorption capacity of 394.88 $mg.g^{-1}$ at 30 °C. This study has demonstrated that ABA-16, synthesised using HMS as the template and PEG 400 as the carbon source, possessed promising potentials as an adsorbent for the removal of micropollutants from water bodies.

ACKNOWLEDGEMENT

This work was supported by the Government of Malaysia through financial assistances provided by the Fundamental Research Grant Scheme (FRGS) PJK/203/6071330.

REFERENCES

1. Peng, X., et al., *Preparation of a graphitic ordered mesoporous carbon and its application in sorption of ciprofloxacin: Kinetics, isotherm, adsorption mechanisms studies.* (Microporous and Mesoporous Materials, 2016). **228**: p. 196-206.
2. Qin, L., et al., *Novel N-doped hierarchically porous carbons derived from sustainable shrimp shell for high-performance removal of sulfamethazine and chloramphenicol.* (Journal of the Taiwan Institute of Chemical Engineers, 2016). **62**: p. 228-238.
3. Huang, X., S. Wu, and X. Du, *Gated mesoporous carbon nanoparticles as drug delivery system for stimuli-responsive controlled release.* (Carbon, 2016). **101**: p. 135-142.
4. Tripathi, P., et al., *Mesoporous Carbon Nanomaterials as Environmental Adsorbents*. Vol. 14. (2014). 1823-37.
5. Zhu, Z., et al., *A three-dimensional ordered mesoporous carbon/carbon nanotubes nanocomposites for supercapacitors.* (Journal of Power Sources, 2014). **246**: p. 402-408.
6. Zhang, B., et al., *Synthesis of ordered mesoporous carbon using m-Diethynylbenzene as a new precursor.* (Materials Letters, 2017). **189**: p. 317-320.
7. Guo, R., et al., *Synthesis and surface functional group modifications of ordered mesoporous carbons for resorcinol removal.* (Microporous and Mesoporous Materials, 2013). **175**: p. 141-146.
8. Gokulakrishnan, N., et al., *An ordered hydrophobic P6mm mesoporous carbon with graphitic pore walls and its application in aqueous catalysis.* (Carbon, 2011). **49**(4): p. 1290-1298.
9. Zhao, D., et al., *Triblock Copolymer Syntheses of Mesoporous Silica with Periodic 50 to 300 Angstrom Pores.* (Science, 1998). **279**(5350): p. 548.
10. Sudaryanto, Y., et al., *High surface area activated carbon prepared from cassava peel by chemical activation.* (Bioresource Technology, 2006). **97**(5): p. 734-739.
11. Jia, Q. and A.C. Lua, *Effects of pyrolysis conditions on the physical characteristics of oil-palm-shell activated carbons used in aqueous phase phenol adsorption.* (Journal of Analytical and Applied Pyrolysis, 2008). **83**(2): p. 175-179.

12. El-Hendawy, A.-N.A., *Variation in the FTIR spectra of a biomass under impregnation, carbonization and oxidation conditions.* (Journal of Analytical and Applied Pyrolysis, 2006). **75**(2): p. 159-166.
13. Lua, A.C. and T. Yang, *Effect of activation temperature on the textural and chemical properties of potassium hydroxide activated carbon prepared from pistachio-nut shell.* (Journal of Colloid and Interface Science, 2004). **274**(2): p. 594-601.
14. Lua, A.C., T. Yang, and J. Guo, *Effects of pyrolysis conditions on the properties of activated carbons prepared from pistachio-nut shells.* (Journal of Analytical and Applied Pyrolysis, 2004). **72**(2): p. 279-287.
15. Karaman, I., et al., *The effect of process parameters on the carbon dioxide based production of activated carbon from lignite in a rotary reactor.* (Fuel Processing Technology, 2014). **118**(0): p. 34-41.
16. Marcilla, A., M. Asensio, and I. Martín-Gullón, *Influence of the carbonization heating rate on the physical properties of activated carbons from a sub-bituminous coal.* (Carbon, 1996). **34**(4): p. 449-456.
17. Alkan, M., et al., *Adsorption kinetics and mechanism of maxilon blue 5G dye on sepiolite from aqueous solutions.* (Chemical Engineering Journal, 2008). **139**(2): p. 213-223.
18. Peng, X., et al., *Adsorption of anionic and cationic dyes on ferromagnetic ordered mesoporous carbon from aqueous solution: Equilibrium, thermodynamic and kinetics*. Vol. 430C. (2014). 272-282.